High-frequency behavior of quantum-based devices: Equivalent-circuit, nonperturbative-response, and phase-space analyses

F. A. Buot and A. K. Rajagopal
Naval Research Laboratory, Washington, D.C. 20375
(Received 28 June 1993)

The high-frequency response of resonant tunneling devices (RTD's), subjected to a time-dependent signal, is considered in two different situations when operating in the negative-differential-resistance (NDR) region: stable and unstable. The study of this behavior is considered from three different approaches, all based on the phase-space distribution-function formalism. In the stable case, the equivalent-circuit approach (ECA) is deduced from the published numerical results obtained by one of us (F.A.B. and collaborators) dealing with the complex dynamical aspects in phase space of quantum transport in RTD, operating at dc bias in the NDR region of its ideal characteristic current-voltage (I-V) curve. The ECA is found to be very useful in resolving the various outstanding controversies concerning the dynamical quantum transport behavior of RTD. For unstable operation in the NDR region, nonperturbative approaches are more appropriate. Here, a time-dependent transformation of phase space is found which transforms the quantum distribution (QDF) transport equation to the same form as that in the absence of a time-dependent signal. This time-dependent transformation is useful when the applied time-dependent electric field is assumed to be position independent. In a more general and realistic situation, an applied time-dependent voltage at the drain will self-consistently lead to a time-dependent and position-dependent potential inside the device. For this general situation, we introduce two different representations of quantum transport, namely, the Liouville representation and the phase-space fluid representation. The QDF solution has inherent undesirable features for studying the dynamics of phase space, which can be eliminated by special processing. This processing yields the positive definite Husimi distribution. It is suggested that the use of the Husimi distribution enables a microscopic dynamical viewpoint of ECA as well as shedding further light on the dynamical nature of the quantum inductance.

I. INTRODUCTION

The time-dependent characterization of quantum transport in resonant tunneling devices (RTD's) has always been plagued with controversies due to the lack of a clear physical picture of the fundamental underlying quantum processes. Notable among these are the long-standing controversy regarding the exact nature of the experimentally measured "time-averaged" I-V characteristics of RTD's, exhibiting a plateaulike behavior and double hysteresis when operating in the negative differential-resistance (NDR) region. There were two schools of thought, with opposing views, trying to explain this characteristic I-V behavior. Goldman, Tsui, and Cunningham[1] attribute the entire behavior to the "intrinsic charge bistability," i.e., charge is built up and eventually become degenerate with a depleted state and is ejected from the quantum well. Theoretical analysis and numerical modeling favoring this viewpoint do exhibit hysteresis, but failed to show any plateaulike behavior. An opposing view was proposed by Sollner,[2] claiming that instead of the bistable charging of the quantum well, I-V behavior is due to externally induced current oscillations. Implied in this circuit viewpoint is the existence of lead inductance. Theoretical analysis favoring Sollner's viewpoint clearly shows that the plateaulike behavior is attainable, but fails to show hysteresis. This confusing state of understanding has only been resolved recently by a fully time-dependent quantum transport numerical simulation from Jensen and Buot.[3] Following this work, Buot and Jensen[4] proposed an equivalent-circuit model for the RTD which accounts for the quantum inductance and nonlinear negative resistor, to explain the controversial I-V behavior, particularly the charge bistability and the presence of the intrinsic current oscillations.

Another major controversy arises from the results of the numerical simulation of the RTD. Indeed, there is much confusion in the literature concerning the frequency-dependent response of the RTD to a small ac signal applied at the terminals. The numerical simulation of Frensley,[5] using a series expansion of the Wigner distribution transport equation (WDFTEQ), reveals a capacitive behavior at lower frequencies changing into an inductive behavior at higher frequencies. In contrast, the numerical simulation of Kluksdahl *et al.*,[6] using a similar WDFTEQ approach, applying a step voltage pulse across the NDR region, and using a Fourier transformation, reveals inductive behavior at low frequencies, changing into a capacitive behavior at intermediate frequencies, and eventually displaying somewhat inductive behavior at high frequencies. Both these simulations qualitatively agree concerning the real part of the admittance, namely that it is negative at lower frequencies and becomes positive at higher frequencies. Their results also concur at very high frequencies by having a cutoff in the admittance. Until now the discrepancy in the reactive behavior cited above has remained unresolved.

So far, there has been no other serious work on the

0163-1829/93/48(23)/17217(16)/$06.00

subject of characterizing the high-frequency response of the RTD to an ac signal, although there have been a number of attempts to analyze the high-frequency behavior of nanometric structures. These are attempts to extend the Landauer-Buttiker viewpoint, which calculates conductance from transmission coefficients to high frequencies. The gross deficiencies of all these attempts have been discussed by Landauer.[7] There are also attempts, for example by Fu and Dudley,[8] which employ the machinery of the linear-response theory for noninteracting systems; however, this particular approach is plagued by its inability to treat far-from-equilibrium operating bias conditions, of interest to the nanoelectronics community. A different approach using an analytical path integral method based on the nonequilibrium Green's function was proposed by Chen and Ting.[9] This does not include self-consistency, and seems to be complementary to the non-self-consistent WDFTEQ numerical approach of Frensley,[5] in view of the comparison made of their results with Frensley's and with experimental values. However, their result for the imaginary part of the admittance is inductive at low frequencies, in contradiction to the more recent result by Frensley,[5] which correctly shows capacitive behavior at these frequencies. Moreover, none of the general features of the imaginary part of the admittance mentioned above is contained in their results. Thus their result for NDR stands alone, and points to fundamental differences between their approach and Frensley's. More recent results from Cai and Lax[10] employ a nonperturbative time-dependent Green's function approach to compute the behavior of an electron incident from an energy channel on a double-barrier structure. Their results reveal the presence of intrinsic oscillations in response to a voltage pulse across the negative-differential-resistance (NDR) region, similar to the result obtained by Buot and Jensen,[11] particularly when self-consistency and scattering were switched off in their WDFTEQ calculations. The results of Cai and Lax, however, are limited to single-channel and non-self-consistent contributions.

The purpose of this paper is to show that a coherent and unified understanding of the high-frequency linear-response behavior of the RTD arises from the equivalent-circuit model of Buot and Jensen (BJ),[4] referred to here as the BJ model (originally proposed to study the nonlinear aspects of the RTD which arise from quantum nonlocality and the self-consistent treatment of WDFTEQ, including scattering, which is referred to here as the QDF approach), and to point out a proper way to a nonperturbative theoretical framework for analyzing the high-frequency behavior of resonant tunneling devices within the quantum distribution-function approach. We also show that the BJ model (and its modification at high frequencies to take into account the electron inertia) may be justified from the fundamental QDF transport equation by appropriate partitioning of phase space in calculating the tunneling and displacement currents. It is worthwhile to stress this point here since there have been misleading statements in the literature claiming that no understanding exists for quantum transport at nonzero frequencies. Also, there is a need to clarify a statement made in the literature[8] which strongly implies that no inductance (L)-resistance (R)-capacitance (C) (LRC) circuitry can simulate the complicated frequency dependence of the admittance in the linear-response regime, particularly since this statement is made without further reservations. We will show here that the two numerical simulations mentioned above[5,6] may be recast in terms of the BJ model corresponding to two separate regimes in the BJ circuit parametrization, operating in the NDR region. Moreover, these two regimes are also different from the parametrization used by BJ to resolve the controversial I-V characteristic of the RTD. Thus the BJ model is found to be the basic equivalent-circuit model of the RTD; it includes the high-frequency behavior of the RTD more accurately, if one adds a smaller series inductance to be discussed below.

A nonperturbative treatment of the RTD response to a small ac signal, biased in the middle of the NDR region, becomes a necessity in the regime of circuit parametrization of the BJ model used to explain the experimental time-averaged I-V characteristic of a symmetric double-barrier structure. In this regime, the middle of the NDR becomes an unstable point, which means that a small perturbation generally leads to large nonlinear effects, rendering the linear approach invalid. In this paper, a nonperturbative theoretical framework for analyzing the high-frequency response of the RTD within the QDF approach is formulated.

The study of the structure of phase space in nonlinear quantum transport characterization of the RTD was initiated by Buot and Jensen.[11] Indeed, quantum phase-space theories have provided an attractive approach to the study of nonlinear quantum phenomena, such as quantum chaos, and their correspondence to classical nonlinear phenomena. It provides a proper setting for studying nonlinear dynamics through the structure of phase space (trajectory and "contour" analysis). An initial study of the structure of the phase space of an open system by means of the Wigner trajectories, subjected to different voltage bias, has been reported by Buot and Jensen.[11] In their work, difficulties in calculating the Wigner trajectories were encountered at the current peak where the WDF oscillates violently within the device. In the present paper, we propose to study the structure of phase space through the QDF approach for simulating the RTD by a Gaussian smoothing of the numerically obtained WDF to calculate quantum trajectories. It should be mentioned that this smoothing does not alter the basis of the QDF theory, as it is actually an alternative to the Wigner distribution theory and has been successful in elucidating the quantum dynamics of classically chaotic motion in a double-well potential.[12] For an operating bias that does not lead to a violently oscillating WDF, the smoothing procedure does not alter the WDF. This phase-space analysis is discussed in this paper.

The outline of this paper is as follows. In Sec. II, we describe the equivalent-circuit representation of the RTD and describe in detail the result of such a characterization, particularly the resolution of the controversy regarding the reactive behavior of the RTD. In Sec. III, we introduce the time-dependent transformation of phase

space in order to address the problem of time-dependent but position-independent applied external electric field. In Sec. IV, the processing of the QDF for the study of the structure and dynamics of phase space is developed. Concluding remarks are given in the Sec. V.

II. THE EQUIVALENT-CIRCUIT REPRESENTATION OF THE RTD

An exact QDF transport equation is derived, and applied to the RTD together with the subsidiary device boundary condition, by Buot and Jensen.[11] A simplification of the QDF transport equation was used[11] in simulating RTD's, based on the effective-mass approximation and retaining only the leading collision terms. In the relaxation-time approximation for the leading collision terms, the resulting equation for the QDF is given as

$$\frac{\partial f_w(\mathbf{p},\mathbf{q},t)}{\partial t}=\frac{-\mathbf{p}}{m^*}\cdot\nabla_q f_w(\mathbf{p},\mathbf{q},t)+\frac{2\pi}{h^4}\int d\mathbf{p}'d\boldsymbol{\nu}\{V(\mathbf{q}-\boldsymbol{\nu}/2)-V(\mathbf{q}+\boldsymbol{\nu}/2\}\sin\left[\frac{(\mathbf{p}-\mathbf{p}')\cdot\boldsymbol{\nu}}{\hbar}\right]f_w(\mathbf{p}',\mathbf{q},t)$$
$$+\frac{1}{\tau}\left\{\frac{\rho(\mathbf{q},t)f_0(\mathbf{p},\mathbf{q})}{\rho_0(\mathbf{q})}-f_w(\mathbf{p},\mathbf{q},t)\right\}, \tag{1}$$

where $\rho(\mathbf{q},t)=1/h^3\int d\mathbf{p}f_w(\mathbf{p},\mathbf{q},t)$ is the particle density, $f_0(\mathbf{p},\mathbf{q})$ is the equilibrium WDF, and τ is the average relaxation time calculated by considering all the scattering processes and using Matthiessen's rule. The above equation must then be solved together with the Poisson equation, namely,

$$\nabla^2\phi(\mathbf{q})=[e\rho(\mathbf{q},t)-en_0(\mathbf{q})]/\epsilon\ , \tag{2}$$

where $en_0(\mathbf{q})$ represents the background charge density. Therefore $V(\mathbf{q})$ is given by

$$V(\mathbf{q})=\phi(\mathbf{q})+\Delta E_c(\mathbf{q})\ . \tag{3}$$

$f_w(\mathbf{p},\mathbf{q},t)$ is the familiar Wigner distribution function (WDF), and m^* is the effective mass of the electron. ΔE_c is usually determined empirically from the band-edge discontinuities at the heterojunction interfaces.

Using a subsidiary boundary condition, the above simplification was used by Jensen and Buot[3] to simulate a symmetrical double-barrier structure shown in Fig. 1. It consists of an undoped buffer-barrier-quantum-well-barrier-buffer region sandwiched between two heavily doped regions. The time-averaged I-V characteristic is shown in Fig. 2, where the non-self-consistent (i.e., voltage is linearly dropped across the undoped region only) I-V result is also shown for comparison. The presence of a series resistor can immediately be observed from comparison of the two I-V plots. This series resistance R can be estimated to be equal to the voltage difference of the location of the two current peaks divided by the value of the current peak of the self-consistent I-V result. The presence of this resistor is critical since together with the capacitance C across the undoped region it creates delay in bringing a supply of electrons from the reservoir to the barrier edge. The accumulated charge at the barrier edge would then leak through the double-barrier region via tunneling.

Thus there are basically two characteristic times that control the current flow in a symmetric RTD, operating in the NDR region. The first is referred to here as the charge buildup time τ_B, and the second is referred to as the charge leakage time τ_L. The charge buildup time τ_B is the time it takes to build up the charge of the electrons from the particle reservoir to the emitter-barrier edge in response to the increase of voltage bias at the collector terminal. This is measured by the product of the series resistance R and the capacitance of the undoped region

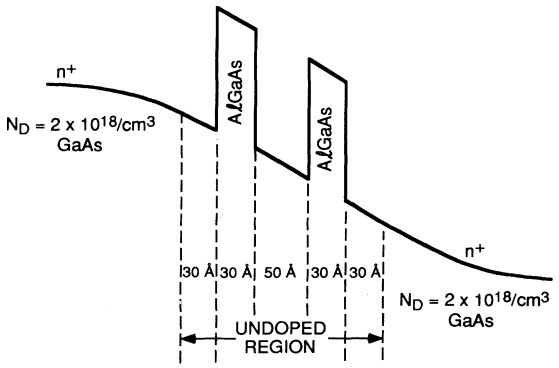

FIG. 1. Schematic band-edge diagram of the RTD under bias simulated by the QDF approach, and used to derive the BJ circuit model.

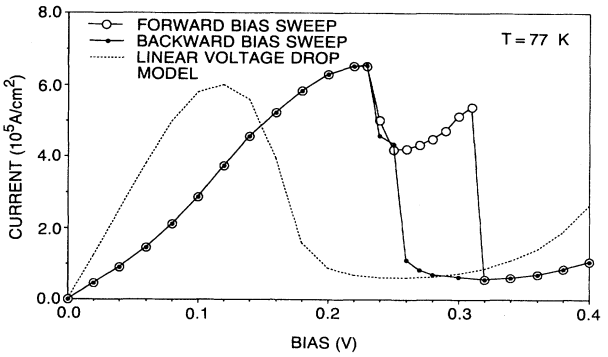

FIG. 2. Current as a function of applied bias. "Linear drop" refers to (non-self-consistent) simulations in which the bias was assumed to linearly decrease across the quantum-well region (Ref. 3). The NDR region occurs between biases of 0.23 and 0.32 V.

consisting of the buffer-barrier-well-barrier-buffer layers. The charge leakage time τ_L is more complicated since it reflects the nonlinearity of the quantum transport through the double-barrier structures. When the Fermi level of the source (emitter) is above the quantum-well resonant-energy level, it is the time it takes to charge the quantum well by tunneling through the first barrier, so that by virtue of self-consistency, the resonant-energy level becomes aligned with the Fermi level of the source, allowing the tunneling current to increase to a maximum. Thus the tunneling current would typically lag behind the increase in the voltage drop across the double-barrier region. However, the rather slow readjustment of the charge buildup in the emitter region will eventually catch up resulting in the Fermi level lying below the resonant-energy level of the quantum well, with attendant overshoot in the alignment between the two levels. On the other hand, when the Fermi level of the source is lying below the resonant-energy level of the quantum well, the tunneling-leakage time through the second barrier measures the charge depletion process in the quantum well, which together with the action of self-consistency, leads toward realignment of the resonant-energy level with the Fermi level of the source (emitter), allowing the tunneling current to increase to a maximum. However, the slow readjustment of the charge in the emitter region to replace the charge will eventually result in the overshoot of the alignment of the two energy levels, with the Fermi level of the source lying above the resonant-energy level of the quantum well. This process then repeats, and oscillations occur. It is clear that for a symmetric double-barrier structure, the discharging and charging tunneling times are equal, with the corresponding processes being inherently not in phase, i.e., one necessarily follows somewhat after the other. Since the charging and discharging of the quantum well reflects the tendency to maintain ("to correct") the alignment of the Fermi level of the emitter with the resonant-energy level of the quantum well, the oscillatory behavior results from the overshoot of the energy-level alignment and the highly correlated discharging and charging of the quantum well, by virtue of the longer buildup times of the charge at the barrier edge compared to the leakage tunneling time. This means that for $\tau_B > \tau_L$ (this condition will be discussed in more detail later), the alignment of the resonant-energy level of the quantum well relative to the Fermi level of the source oscillates, for the RTD operated in the NDR region. Indeed, this phenomena is unambiguously demonstrated by the numerical simulation of the RTD using the "quantum Monte Carlo" particle technique.[13]

The resulting current oscillations have been demonstrated by Jensen and Buot,[3] using the QDF approach discussed above. The fact that the tunneling current contribution to the total current has an inductive character led Buot and Jensen[4] to propose the BJ model for the equivalent circuit of the RTD operating in the NDR region, which incorporates the quantum inductance L in series with the nonlinear negative conductance G. In the BJ model, τ_L is measured by the product of an inductance L, which is referred to as the quantum inductance, and the absolute value of the negative conductance G. The total current is the sum of the inductive tunneling current, $T(t)$, plus the rate of change of the polarized charge across the RTD structure. This is the time-dependent displaced charge Q_D of the doped region at the drain side.[4] Therefore, we have the total time-dependent current $I(t)$, given as

$$I(t)=T(t)+\dot{Q}_D \ , \tag{4}$$

which immediately suggests the presence of an equivalent circuit representing the undoped region, consisting of an inductive branch parallel to a capacitive branch. Since the inductive branch is solely responsible for the conduction when the current does not oscillate, i.e., when the series resistor R is small enough such that $\tau_B < \tau_L$, it becomes easy to deduce that the inductive branch consists of the inductive element L and a nonlinear resistor characterized by the $i(v)$ relation of the non-self-consistent linear-drop model of Fig. 2.

Thus the basic BJ model of a RTD operating in the NDR region derived from the fundamental consideration of the quantum transport across a double-barrier structure has four independent equivalent-circuit parameters: the series resistance R, a nonlinear resistor characterized by a negative conductance G, quantum inductance L, and capacitance C. This is shown in Fig. 3. As indicated above, the RTD simulated by BJ, with fixed bias applied in the NDR, is characterized by the following inequalities for the circuit parameters: $R|G|>1$ and $RC>L|G|$. $RC>1$ roughly means that a relatively large amount of

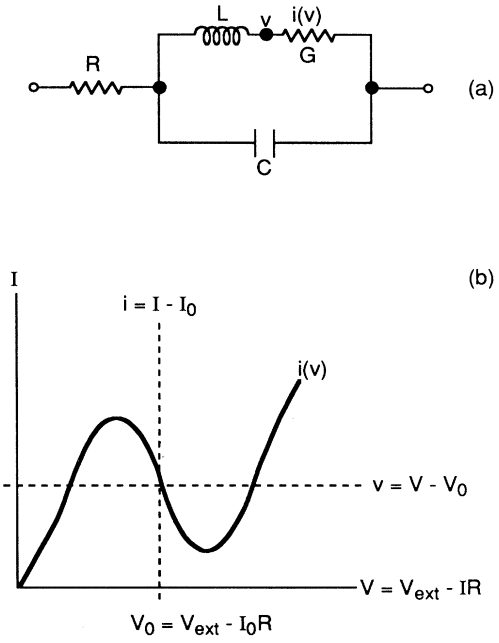

FIG. 3. (a) The basic BJ equivalent-circuit model of the RTD at low frequencies. It is derived from the numerical simulation of the QDF transport equation (Ref. 4). This was used by BJ to resolve the controversy regarding the intrinsic bistability of the RTD, operating in the NDR region. (b) Transformation of current and voltage variables used in the circuit equations.

charge has to be moved in the emitter region from the reservoir corresponding to a small change in the resonant-energy level. This would enhance the charge buildup time τ_B in the emitter region. These are conditions for the presence of oscillatory behavior and instability of the operating point in the middle of the NDR region[3,4] leading to the intrinsic bistability and hysteresis in the current-voltage characteristics, which were the focus of the original BJ model. In contrast, we now find that the RTD's simulated by Frensley[5] and Kluksdahl *et al.*[6] are obtained if the following inequalities are obeyed: $R|G|<1$ and $RC<L|G|$, along with further conditions to be specified in what follows. The above are conditions for the nonoscillatory and stable operation in the middle of the NDR region allowing for the applicability of linear-response approximation.[4] They also imply that the series resistance is quite small compared to that of the RTD simulated by BJ (note that the RTD simulated by BJ, although having approximately the same feature sizes for the double-barrier region, differs in having an undoped buffer layer on both sides of the double barrier, which may also affect the value of the capacitance relative to those of Refs. 5 and 6, and a longer computational box length, which together introduces a larger R). Moreover, the RTD simulated by Frensley,[5] without taking self-consistency into account, differs from that simulated by Kluksdahl *et al.*,[6] which takes self-consistency into account, by the following inequality: $L|G|<C/|G|$ for Frensley,[2] whereas $L|G|>C/|G|$ for Kluksdahl *et al.*[6] These imply a larger quantum inductance for the RTD of Ref. 6 as compared to that simulated in Ref. 5. The residual small inductance in Frensley's case is due mainly to quantum reflections and nonlocality. This means that the current response lags behind the change in the applied voltage due to quantum reflections at the interfaces and large distance readjustments of the wave function. This is supported by the numerical simulation in which an oscillatory current response results from the application of a step voltage pulse across the NDR region, without taking self-consistency into account. This situation is only true for operating bias in the NDR region, by virtue of the fact that it takes some time for the wave function to spread out across the quantum well, with the aid of a reflection-mediated readjustment to effectively raise the resonant-energy level out of the triangular potential region of the deformed quantum well. There is no readjustment of the Fermi level in the emitter region in the absence of self-consistency, so that alignment overshoot and self-oscillations cannot be supported at fixed bias in the NDR region. Further, note that Ref. 6 uses wider barrier widths than those used in Ref. 5 and BJ, and furthermore, that BJ use an undoped buffer layer at each side of the double-barrier region. All these will affect their actual respective capacitance and series resistance. From the discussion of this paragraph, the BJ circuit model serves not only to clarify the origin of the discrepancy of the results of the two numerical simulations,[5,6] but also to bring together the various dynamical aspects of the RTD in terms of WDFTEQ.

In addition to the quantum inductance, found by BJ to be parallel to the capacitance for fixed bias in the NDR region, it is important also to take into account effects arising from the electron kinetics in calculating the RTD response to a high-frequency ac signal. These effects are often regarded as due to the electron inertia, i.e., it takes time for the electron to accelerate and decelerate, typically causing the current to lag in time behind the electric field. These inertial effects, although always present, are negligible at low frequencies. It is taken into account in our high-frequency equivalent-circuit model of the RTD by adding another inductance l (l is typically an order of magnitude smaller than the quantum inductance L), in series with R, outside the two-branch circuit of L, G, and C. This is shown in Fig. 4. As will be shown in the following figures, this additional "inertial inductance" l serves to cut off the RTD response at very high frequencies.

A. Calculation of the complex admittance of the RTD: Linear response

To calculate the complex-value admittance, let us assume that a small complex-valued ac signal given by $v_0 e^{i\omega t}$ is applied across the two terminals of the RTD. For a stable perturbation around the middle of the NDR region, we can approximate the current in the nonlinear resistor in Fig. 3 to be given by

$$i(v)=Gv \ . \tag{5}$$

Then the equation for the voltage drop v measured from the middle of the NDR region across the nonlinear resistor is given by the following linear circuit equation:

$$RCLG\ddot{v}+(RC+LG)\dot{v}+(RG+1)v=v_0 e^{i\omega t} \ . \tag{6}$$

For the calculating the current response, we are only interested in the particular solution of Eq. (6). This is given by

$$v=v_0 e^{i\omega t}/\{[(RG+1)-\omega^2 RCLG]+i\omega(RC+LG)\} \ . \tag{7}$$

The terminal current response, $\Delta i(t)=\Delta i_c+\Delta i_L$ in the equivalent-circuit model of Fig. 3 is obtained as

$$\Delta i(t)=CLG\dot{v}+C\dot{v}+Gv \ . \tag{8}$$

Upon substituting the particular solution for v in Eq. (8), we are led to the following expression for the complex admittance:

$$\sigma(\omega)=\mathrm{Re}\sigma(\omega)+i\ \mathrm{Im}\sigma(\omega) \ , \tag{9}$$

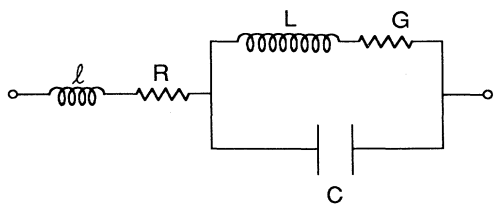

FIG. 4. An equivalent-circuit model of the RTD for calculating the high-frequency signal response. It is used here to resolve the controversy concerning the reactive behavior of the RTD.

where

$$\mathrm{Re}\sigma(\omega)=\frac{1}{RCLG}\left\{\frac{G(1-\omega^2CL)(\omega_0^2-\omega^2)+\omega^2C\eta}{(\omega_0^2-\omega^2)^2+(\omega\eta)^2}\right\}, \tag{10}$$

$$\mathrm{Im}\sigma(\omega)=\frac{\omega}{RCLG}\left\{\frac{C(\omega_0^2-\omega^2)-G(1-\omega^2CL)\eta}{(\omega_2^2-\omega^2)^2+(\omega\eta)^2}\right\}. \tag{11}$$

The expressions for ω_0^2 and η are given in terms of the equivalent-circuit parameter as

$$\omega_0^2=(RG+1)/RCLG\ , \tag{12}$$

$$\eta=(RC+LG)/RCLG\ . \tag{13}$$

We immediately observe that if $\mathrm{Re}\sigma(\omega)$ represents a negative conductance at $\omega=0$, as found by Frensley[5] and Kluksdahl *et al.*,[6] then $RG+1>0$ or $R|G|<1$. This is consistent with our previous assumption regarding the smallness of R in Refs. 5 and 6 compared to BJ. This also implies that the parameter $\omega_0^2<0$. Since R is small, then the parameter $\eta>0$ for similar reasons. In the limit ω become very large, the inductive element blocks the effect of the negative resistor, $\mathrm{Re}\sigma(\omega)$ becomes positive and is asymptotically given by $1/R$, a finite limit in the absence of the effects of the electron inertia discussed above. Therefore $\mathrm{Re}\sigma(\omega)$ must cross the frequency axis at some particular value ω_c. The crossing frequency is given by the smallest positive root of the following equation:

$$|G|(1-\omega^2CL)(|\omega_0^2|+\omega^2)+\omega^2C\eta=0\ . \tag{14}$$

This is a quadratic equation in $y=\omega^2$. One positive root is guaranteed; this is the crossing frequency ω_c given by

$$\omega_c=\{\alpha\pm\sqrt{\alpha^2+\gamma^2}\}^{1/2}\ , \tag{15}$$

where

$$\alpha=\{|G|+C\eta-|G||\omega_0^2|CL\}/(2|G|CL)\ , \tag{16}$$

$$\gamma=\left[\frac{|\omega_0^2|}{CL}\right]^{1/2}. \tag{17}$$

Clearly, when a smaller inductance due to the effects of the electron inertia is also taken into account, at least an extrema of $\mathrm{Re}\sigma(\omega)$ exists for another positive value of w. These results are indeed what was observed in the WDF numerical simulation of Frensley[5] and Kluksdahl *et al.*[6]

The imaginary part $\mathrm{Im}\sigma(\omega)$ is proportional to ω at low frequencies. It is inductive at low frequencies provided $L|G|>C/|G|$ holds. Otherwise, $\mathrm{Im}\sigma(\omega)$ is capacitive. At low frequencies, Kluksdahl *et al.*[6] found $\mathrm{Im}\sigma(w)$ to be inductive, whereas Frensley[5] found it to be capacitive. This supports our claim that the neglect of the self-consistency in Ref. 5 resulted in a much smaller quantum inductance compared to that of Ref. 6, where self-consistency was taken into account. In all cases, at higher frequencies, the quantum inductance ceases to contribute to the reactive component, as expected, and $\mathrm{Im}\sigma(\omega)$ is always positive and characterized by the RC branch of the equivalent circuit, i.e.,

$$\mathrm{Im}\sigma(\omega)|_{\omega\to\infty}=\frac{1}{R^2\omega C}\ . \tag{18}$$

It is interesting to note that when the following condition is satisfied, namely $L|G|>C/|G|$, then a positive frequency ω_c^I for crossing from the inductive to capacitive behavior exists and is given by

$$\omega_c^I=\left\{\frac{L|G|^2-C}{RCL|G|(|G|CL\eta+C)}\right\}^{1/2}. \tag{19}$$

The above finite asymptotic capacitive limit is only true if the inductive effect due to the electron inertia is not taken into account. Otherwise, another crossing of the frequency axis from capacitive to inductive behavior also exists, with the inductive behavior asymptotically going to zero at very high frequencies. This analytical result agrees with the numerical simulation of Kluksdahl *et al.*[6] On the other hand, if $L|G|<C/|G|$ as in the numerical simulation of Frensley,[5] then crossing of the frequency axis should be absent, unless a smaller inductance (roughly one order of magnitude less than the quantum inductance) due to the electron inertia in series with the RTD circuit of Fig. 3 is also taken into account, which will lead to crossing from capacitive to inductive behavior and asymptotically going to zero at very high frequencies. These considerations are indeed in conformity with Frensley's numerical result.

In the presence of the inertial inductance l, the expression for the real and imaginary parts of the admittance become

$$\mathrm{Re}\sigma(\omega)=\frac{1}{RCLG}\left\{\frac{G(1-\omega^2CL)[\omega_0^2-(1+\delta)\omega^2]+\omega^2C(\eta+\delta\eta)}{[\omega_0^2-(1+\delta)\omega^2]^2+[\omega(\eta+\delta\eta)]^2}\right\}, \tag{20}$$

$$\mathrm{Im}\sigma(\omega)=\frac{\omega}{RCLG}\left\{\frac{C[\omega_0^2-(1+\delta)\omega^2]-G(1-\omega^2CL)(\eta+\delta\eta)}{[\omega_0^2-(1+\delta)\omega^2]^2+[\omega(\eta+\delta\eta)]^2}\right\}, \tag{21}$$

where the "correction terms" are given by

$$\delta=\frac{l}{L}\frac{1}{RG}\ , \tag{22}$$

$$\delta\eta=\frac{l}{L}\frac{1}{RC}-\frac{l}{R}\omega^2\ . \tag{23}$$

Figure 5 shows the result of the calculations employing the parametrization of the BJ model discussed above, characterizing the non-self-consistent RTD numerical simulation of Frensley,[5] without taking into account the inertial inductance l. In this figure the value of the circuit parameters are chosen such that $R|G|<1.0$,

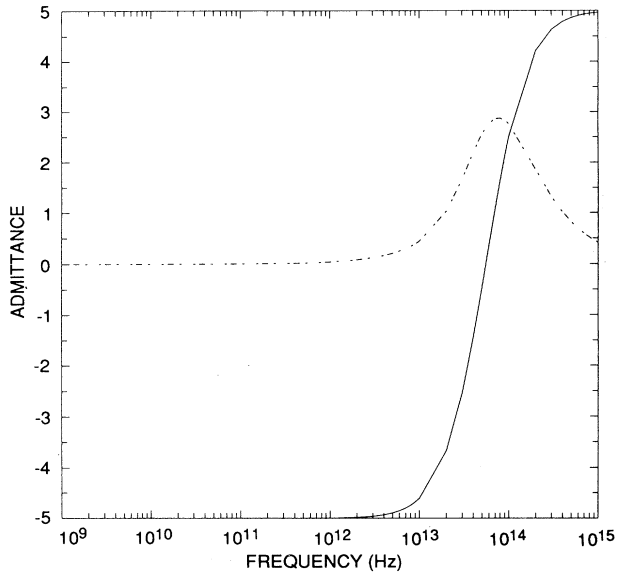

FIG. 5. Small signal response employing the parametrization of the BJ circuit model characterizing the non-self-consistent RTD numerical simulation of Frensley (Ref. 5): $R|G|<1.0$, $RC<L|G|$, and $L|G|<C/|G|$. The values used are $R=0.2\times10^{-7}$ $\Omega\,\mathrm{cm}^2$, $G=-2.5\times10^{7}$ S/cm^2, $C=6.0\times10^{-7}$ F/cm^2, and $L=0.8\times10^{-21}$ H cm^2.

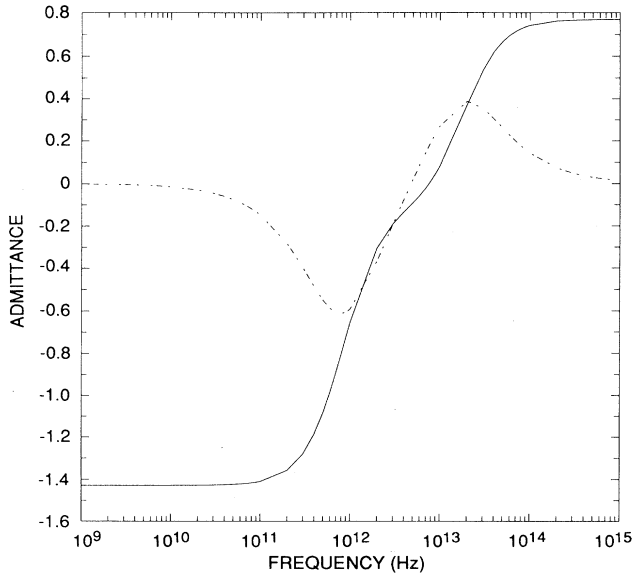

FIG. 7. Small signal response for another set of BJ circuit parameters characterizing the self-consistent RTD simulation of Kluksdahl *et al.* (Ref. 6), with zero inertial inductance: $R|G|<1.0$ $RC<L|G|$, and $L|G|>C/|G|$. The values used are $R=1.3\times10^{-7}$ $\Omega\,\mathrm{cm}^2$, $G=-0.5\times10^{7}$ S/cm^2, $C=0.4\times10^{-6}$ F/cm^2, and $L=9.0\times10^{-20}$ H cm^2.

$RC<L|G|$, and $L|G|<C/|G|$. Figure 6 shows the result of the calculation for the same set of BJ circuit parameters with the addition of a smaller inertial inductance, l ($l=0.2L$), leading to a cutoff in the admittance at high frequencies. Indeed, in Fig. 6 the characteristic behavior of the complex admittance obtained by Frensley is reproduced.

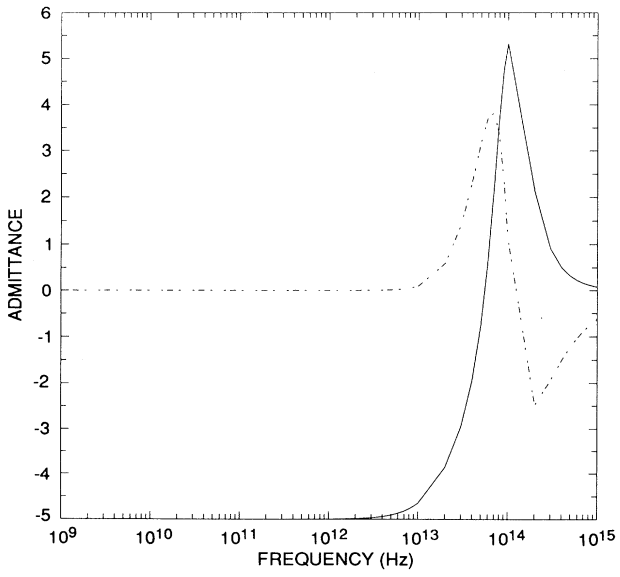

FIG. 6. Small signal response using the same set of BJ circuit parameters as in Fig. 5 but with the addition of smaller inertial inductance, $l=0.2$ L, leading to the cutoff at high frequencies.

Figure 7 shows the result of the admittance calculations for another set of circuit parameters characterizing the self-consistent RTD simulation of Kluksdahl *et al.*[6] with $l=0$. The circuit parameters are chosen such that $R|G|<1$ and $RC<L|G|$, the same relations as those characterizing Frensley's, but with a different relation for $L|G|>C/|G|$. Figure 8 shows the result of the admittance calculations for the same set of parameters as Fig.

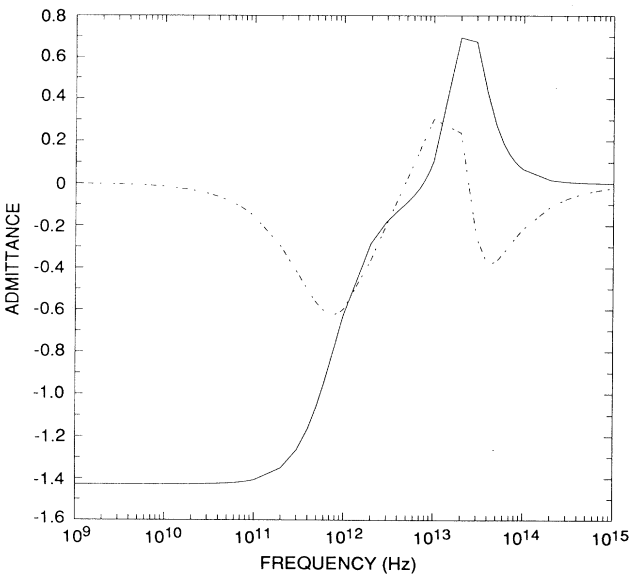

FIG. 8. Small-signal response using the same set of BJ circuit parameters as in Fig. 7, but with inertial inductance, $l=0.05$ L.

7, but taking into account the presence of a smaller inertial inductance l which is about an order of magnitude smaller than the quantum inductance L. The agreement with the characteristic features of the numerical results of Kluksdahl *et al.* is quite good. The agreement of all the calculations can be made more accurate quantitatively by optimizing the five circuit parameters (e.g., using the numerical Levenberg-Marquardt algorithm[14]), subject to the constraints given above, so as to produce the exact crossings and points of extrema. The optimization is not done in this paper, since our immediate goal is to demonstrate the dominant role of the different regimes of the BJ circuit parametrization on the high-frequency qualitative behavior of RTD, and to confirm the basic nature of the BJ equivalent-circuit model for the RTD.

B. Calculation of the complex admittance of the RTD: Nonlinear response

A more realistic treatment of the RTD is to consider the source and drain resistance to be larger than the absolute magnitude of the inherent negative differential resistance in the middle of the NDR region. This was achieved in the QDF numerical simulation of Jensen and Buot[3] by using a longer simulation box length. Self-consistency and scattering, through the use of the relaxation-time approximation,[11] were taken into account. The criteria for oscillations and limit cycle operation in the NDR region were achieved at low temperatures as discussed in Ref. 3, with results in excellent agreement with the experiments.

For a NDR operation which exhibits oscillations and limit-cycle behavior, resulting in hysteresis and charge bistability in the averaged I-V characteristic, the middle of the NDR region, $v=0$, is an unstable point. Therefore, it is no longer valid to use the linear approximation to the current across the nonlinear resistor. Any small perturbation will bring the values of v to large excursions. Thus the problem becomes highly nonlinear. To give the problem a definite form, let us approximate the $i(v)$ characteristic of the nonlinear resistor by adding a cubic term as dictated by the symmetry in Fig. 3, given by

$$i(v)=Gv+\beta v^3 , \tag{24}$$

where β may be approximated as

$$\beta=|G|/3v_p . \tag{25}$$

The quantity v_p is the voltage, measured from the middle of the NDR region, where the current peak is located. Let us take a real ac small signal given by $v_0\cos(\omega t)$ applied across the terminals of the RTD. Then the equation for the voltage drop across the nonlinear resistor, measured from the middle of the NDR region, is given by

$$\ddot{v}+\eta(v)\dot{v}+\zeta(v)\dot{v}^2+\omega_0^2(v)v=\Omega(v)\cos(\omega t) , \tag{26}$$

where

$$\eta(v)=(RC+LG+3\beta Lv^2)/D(v) , \tag{27}$$

$$\zeta(v)=12\beta RCLv/D(v) , \tag{28}$$

$$\omega_0^2(v)=(RG+1+\beta v^2)/D(v) , \tag{29}$$

$$D(v)=RCLG+3\beta RCLv^2 , \tag{30}$$

$$\Omega(v)=v_0/D(v) . \tag{31}$$

Equation (25) is a highly nonlinear equation, and represents a nonlinearly driven nonlinear-damped oscillator. Furthermore, the additional smaller inductance due to the electron inertia in series with the two-branch RTD equivalent circuit could add further complications. The problem requires the analytical and geometrical tools of nonlinear mechanics[15] for its numerical solution.

We should point out that there have been a few attempts in the literature aimed at characterizing the quantum inductance of the RTD. Notably, these are attempts which employ linear-response theory and do not treat the far-from-equilibrium operating bias condition. The result presented here is a by-product of the time-dependent self-consistent QDF approach,[3,4,11] whose value for real device analysis cannot be underestimated.

III. THEORY OF NONPERTURBATIVE SMALL ac SIGNAL RESPONSE OF THE RTD BIASED IN THE NDR REGION

The starting point for the quantum transport equation in the presence of space- and time-dependent perturbation is the QDF transport equation. To simplify the nonperturbative calculation of the small ac signal response, many-body effects are taken into account only to leading order in the expansion in powers of $\hbar$. The derivation of the resulting quantum transport equation in the transformed phase space is outlined in Appendix A for the Hamiltonian in the effective-mass approximation given by $H=\mathbf{p}^2/2m^*+V(\mathbf{q})-\mathbf{f}(t)\cdot\mathbf{q}$. The time-dependent perturbation is $\mathbf{f}(t)\cdot\mathbf{q}$, with $\mathbf{f}(t)$ the position-independent but time-dependent external electric field. At high frequencies, this sort of perturbation is not a bad approximation. For a rigorous numerical treatment of the small ac signal response applied at the drain, one must solve the QDF quantum transport equation and the Poisson equation successively, without the need to assume the form of the perturbation inside the device. This is dealt with in Sec. IV.

In Appendix A, it is shown that the driving term involving $\mathbf{f}(t)$ and its time derivative can be eliminated from the quantum transport equation by making the following transformation in phase space:

$$\mathbf{p}'=\mathbf{p}_0+\int \mathbf{f}(t'')dt'' , \tag{32}$$

$$\mathbf{q}'=\mathbf{q}_0+\xi(t') , \tag{33}$$

where

$$\mathbf{p}_0=\mathbf{p} , \tag{34}$$

$$\mathbf{q}_0=\mathbf{q} , \tag{35}$$

$$\dot{\xi}(t')=\int^{t'}\mathbf{f}(t'')dt'' . \tag{36}$$

In terms of the moving phase space (primed variables), we have

$$\frac{\partial f_w(\mathbf{p}',\mathbf{q}',t')}{\partial t'} = -\frac{\mathbf{p}'}{m^*}\cdot\nabla_q f_w(\mathbf{p}',\mathbf{q}',t') + \frac{1}{\hbar(h/2)^3}\int d\mathbf{p}''d\mathbf{v}\sin\left[\frac{2}{\hbar}(\mathbf{p}'-\mathbf{p}'')\cdot\mathbf{v}\right] \times\{V[\mathbf{q}'-\xi(t')-\mathbf{v}]-V[\mathbf{q}'-\xi(t')+\mathbf{v}]\}f_w(\mathbf{p}'',\mathbf{q}',t') + \frac{1}{\tau}\left\{\frac{\rho(\mathbf{q}',t')}{\rho_0(\mathbf{q}')}f_0(\mathbf{p}',q')-f_w(\mathbf{p}',\mathbf{q}',t')\right\} . \quad (37)$$

We can immediately notice that the last equation written in the moving phase space has exactly the same form as the equation in the absence of the ac signal, which has been used in a number of RTD simulations in Refs. 3 and 11, except for the presence of the driving force in the potential term, in such a manner that one can think of the potential function as moving forward relative to the moving phase space, with velocity $\mathbf{v}(t)=\dot{\xi}(t')=\int^{t'}\mathbf{f}(t'')dt''$. Thus one writes the potential kernel as

$$M[\mathbf{q}'-\xi(t'),\mathbf{p}'-\mathbf{p}''] = \frac{1}{\hbar(h/2)^3}\int d\mathbf{v}\sin\left[\frac{2}{\hbar}(\mathbf{p}'-\mathbf{p}'')\cdot\mathbf{v}\right] \times\{V[\mathbf{q}'-\xi(t')-\mathbf{v}] - V[\mathbf{q}'-\xi(t')+\mathbf{v}]\} . \quad (38)$$

By assuming a harmonic perturbation $\mathbf{f}(t)=\epsilon_0\cos(\omega t)$, then $\xi(t')$ is bounded, oscillatory and small. Thus, from the numerical standpoint, the matrix $M[\mathbf{q}'-\xi(t'),\mathbf{p}'-\mathbf{p}'']$ is simply modified by the oscillatory time dependence (resembling a "back and forth" shaking motion of the potential in the moving phase space) with time t' simply acting as a parameter in the matrix M of the customary time-dependent computer algorithm.

The oscillating time dependence in the matrix M is expected to nonperturbatively modify the form of the results for the QDF obtained in the numerical simulations, as given in Buot and Jensen[11] and Jensen and Buot.[3] Therefore, in the moving phase space, the QDF incorporates the effects of the small ac signal, nonperturbatively, through the oscillating potential matrix M. It follows that the current in the moving phase space would also reveal the effect of the "shaking motion" of the double-barrier potential through the current density $\mathbf{J}(\mathbf{q}',t')$. On the other hand, another time-dependent effect is created by the transformation back to the fixed phase space (laboratory frame), i.e., in the laboratory phase space we have $\mathbf{J}[\mathbf{q}_0+\xi(t),t]$. Thus it is seen to acquire another nonperturbative dependence on time through the $\mathbf{q}_0+\xi(t)$ dependence.

The above discussion leads to the identification of two major nonperturbative effects on the current density. These are (a) effects due to the shaking motion of the effective double-barrier potential as seen by the charge carriers in the moving phase space, and (b) effects due to the transformation of the obtained current density back to the laboratory frame of reference. The first is expected to cause a major complicated change in the intrinsic autonomous oscillatory behavior of the current density, found by Jensen and Buot[3] for the RTD operating in the NDR region, as a function of the frequency of the applied ac signal. We can expect either increased or impeded tunneling rates to occur, resulting in enhancement or quenching of the autonomous intrinsic current oscillations. In a separate context, such phenomena have been found to occur in the quantum transport treatment of a classically known driven-anharmonic oscillator system.[16] The second is expected to cause frequency modulations of the effective intrinsic current oscillations, by virtue of the "swinging back and forth" motion of the current-density wave, as a function of position, across the whole RTD device.

Another way to examine these nonlinear effects is to consider the BJ equivalent circuit for a RTD with a nonlinear negative resistor, which takes into account a series inertial inductance. This has been discussed earlier in Sec. II B.

IV. QUANTUM TRAJECTORIES: PHASE-SPACE PICTURE OF NONLINEAR QUANTUM TRANSPORT

Still another way to study the nonperturbative small ac signal response of the RTD, using the QDF approach, is to search for the quantum particle trajectories in phase space. Buot and Jensen[11] effectively introduce the "Liouville representation" by identifying the QDF transport equation with the following expression:

$$\frac{\partial f_w(\mathbf{p},\mathbf{q},t)}{\partial t} = -\dot{\mathbf{q}}\cdot\nabla_q f_w(\mathbf{p},\mathbf{q},t) - \dot{\mathbf{p}}\cdot\nabla_p f_w(\mathbf{p},\mathbf{q},t) , \quad (39)$$

so that, at steady state, the contour lines of the QDF represents particle quantum trajectories. Note that in this representation the Liouville theorem $df_w(\mathbf{p},\mathbf{q},t)/dt=0$ is satisfied. In the absence of an ac signal, at steady state, Buot and Jensen[11] and Jensen and Buot[17] have reported their study of the Wigner trajectories (contour lines of the QDF). At low bias, these trajectories do seem to have the behavior of real particle trajectories, e.g., they exhibit conservation-of-energy behavior, as well as the expected coherent and incoherent tunneling across a double-barrier structure. However, at very high bias, and particularly at the resonance current peak, the violent fluctuations present in the QDF transport solutions complicate the interpretation of the results and prevent the authors of Refs. 11 and 17 from attaching any meaning to their calculated trajectories. There were also numerical difficulties due to the violent fluctuations, in which the QDF freely takes positive and negative values.

Furthermore, conceptual and numerical difficulties also arise when one tries to define time-evolving trajectories

by calculating the "quantum force" acting on the fictitious particle from Eqs. (1) and (39), as follows:

$$\dot{\mathbf{p}}\cdot\nabla_{\mathbf{p}} f_w(\mathbf{p},\mathbf{q},t) = \frac{2\pi}{h^4}\int d\mathbf{p}'d\boldsymbol{\nu}\left\{V\left[\mathbf{q}-\frac{\boldsymbol{\nu}}{2}\right]-V\left[\mathbf{q}+\frac{\boldsymbol{\nu}}{2}\right]\right\} \times\sin\left[\frac{(\mathbf{p}-\mathbf{p}')}{\hbar}\cdot\boldsymbol{\nu}\right] f_w(\mathbf{p}',\mathbf{q},t) - \frac{1}{\tau}\left\{\frac{\rho(\mathbf{q},t)}{\rho_0(\mathbf{q})} f_0(\mathbf{p},\mathbf{q})-f_w(\mathbf{p},\mathbf{q},t)\right\} . \quad (40)$$

The presence of the gradient of the violently oscillating QDF renders the numerical calculation of the force almost useless. It should be mentioned that even in the absence of scattering and many-body effects, current continuity in phase space is not satisfied in the Liouville representation, unlike in classical systems.

An alternative approach to the calculation of a time-evolving trajectory in phase space and a fictitious quantum force is to enforce the current continuity in phase space by identifying the QDF transport equation with the following expression:

$$\frac{\partial f_w(\mathbf{p},\mathbf{q},t)}{\partial t} = -\nabla_q\cdot\mathbf{J}_q(\mathbf{p},\mathbf{q},t)-\nabla_p\cdot\mathbf{J}_p(\mathbf{p},\mathbf{q},t) , \quad (41)$$

where $f_w(\mathbf{p},\mathbf{q},t)$ is treated as the quantum phase-space density, and the phase-space current densities are given by

$$\mathbf{J}_q(\mathbf{p},\mathbf{q},t) = \frac{\mathbf{p}}{\mathbf{m}^*} f_w(\mathbf{p},\mathbf{q},t) , \quad (42)$$

$$J_{p_\alpha}(\mathbf{p},\mathbf{q},t) = -\frac{1}{h^3}\int d\mathbf{p}'d\boldsymbol{\nu}\left\{V\left[\mathbf{q}-\frac{\boldsymbol{\nu}}{2}\right]-V\left[\mathbf{q}+\frac{\boldsymbol{\nu}}{2}\right]\right\}\cos\left[\frac{(\mathbf{p}-\mathbf{p}')}{\hbar}\cdot\boldsymbol{\nu}\right] f_w(\mathbf{p}',\mathbf{q},t)\Big/\nu_\alpha - \frac{1}{\tau}\int_0^{p_\alpha} dp'_\alpha\left\{\frac{\rho(\mathbf{q},t)}{\rho_0(\mathbf{q})} f_0(\mathbf{p}',\mathbf{q})-f_w(\mathbf{p}',\mathbf{q},t)\right\} . \quad (43)$$

We refer to this approach as the "phase-space fluid representation." The price one has to pay for enforcing the current-continuity equation in phase space is that the QDF do not satisfy Liouville's theorem, even in the absence of many-body effects, unlike the classical systems. The phase-space velocity functions are then defined through the expression

$$\mathbf{J}(\mathbf{p},\mathbf{q},t) = \mathbf{v}(\mathbf{p},\mathbf{q},t) f_w(\mathbf{p},\mathbf{q},t) , \quad (44)$$

where

$$\mathbf{J}(\mathbf{p},\mathbf{q},t) \equiv [\mathbf{J}_p(\mathbf{p},\mathbf{q},t),\mathbf{J}_q(\mathbf{p},\mathbf{q},t)] , \quad (45)$$

$$\mathbf{v}(\mathbf{p},\mathbf{q},t) \equiv [\mathbf{v}_p(\mathbf{p},\mathbf{q},t),\mathbf{v}_q(\mathbf{p},\mathbf{q},t)] . \quad (46)$$

The "dynamical equations" from which trajectories are calculated are taken to be

$$\dot{\mathbf{p}} = \mathbf{J}_{\mathbf{p}}(\mathbf{p},\mathbf{q},t)/f_w(\mathbf{p},\mathbf{q},t) , \quad (47)$$

$$\dot{\mathbf{q}} = \mathbf{J}_{\mathbf{q}}(\mathbf{p},\mathbf{q},t)/f_w(\mathbf{p},\mathbf{q},t) . \quad (48)$$

Numerically, the absence of the gradient of the QDF above is preferable to the definition of the quantum force in the Liouville representation. Note also that the dynamical equations for both the Liouville representation and the phase-space fluid representation are identical when $\mathbf{v}_{\mathbf{q}}(\mathbf{p},\mathbf{q},t)$ is not a function of $\mathbf{q}$, and $\mathbf{v}_p(\mathbf{p},\mathbf{q},t)$ is not a function of $\mathbf{p}$, as in the case of conservative classical systems. However, the equation for $\dot{\mathbf{p}}$ and $\dot{\mathbf{q}}$ cannot be taken strictly as are dynamical equations of the particle trajectory, since the physical interpretation of Eq. (41) as a continuity equation in phase space cannot be taken seriously because the QDF is not positive definite. The numerical difficulties that arise are a result of the violent oscillations of the QDF, preventing us from obtaining numerically well-behaved "point functions" in phase space. Indeed, preliminary calculations of the phase-space "fluid velocities" shows irregular behavior. Therefore, the Wigner trajectory is not suitable for studying the phase-space picture of quantum transport at all bias ranges.

To formulate an appropriate framework for describing the quantum particle trajectories in phase space, it is important to recall that the average value of the position or momentum in the WDF approach obeys effective classical equations of motion by the Ehrenfest theorem. We can reformulate this theorem in the lattice phase-space dynamics, appropriate for our purpose, as follows. In the lattice phase-space quantum dynamics of particles in solids,[18] the time evolution of the expectation value of an arbitrary one-body operator A can be written as

$$\frac{d\langle A(t)\rangle}{dt} = \sum_{\mathbf{p},\mathbf{q},n,n'} \rho_{nn'}(\mathbf{p},\mathbf{q},t)[\hat{H},\hat{A}]_{n'n}(\mathbf{p},\mathbf{q}) , \quad (49)$$

where $\rho_{nn'}(\mathbf{p},\mathbf{q},t)$ is the Weyl transform of the density-matrix operator, n and n' stand for the band and spin indices, and $\hat{H}$ is the single-particle Hamiltonian operator. Substituting the momentum and position operators $\hat{P}$ and $\hat{Q}$ for A, and using the product rule for the Weyl transform of a commutator, we obtain

$$\frac{d\langle\hat{\mathbf{P}}(t)\rangle}{dt} = \sum_{\mathbf{p},\mathbf{q},n,n'} \rho_{nn'}(\mathbf{p},\mathbf{q},t)\frac{\partial H_{n'n}(\mathbf{p},\mathbf{q})}{\partial\mathbf{q}} , \quad (50)$$

$$\frac{d\langle\hat{\mathbf{Q}}(t)\rangle}{dt} = \sum_{\mathbf{p},\mathbf{q},n,n'} \rho_{nn'}(\mathbf{p},\mathbf{q},t)\frac{\partial H_{n'n}(\mathbf{p},\mathbf{q})}{\partial\mathbf{p}} . \quad (51)$$

The two equations above are versions of the Ehrenfest

equations in the lattice Weyl-Wigner formulation of the band theory of solids for arbitrary QDF, $\rho_{nn'}(\mathbf{p},\mathbf{q},t)$. Given an initial position and momentum, the last two equations define a time-dependent particle quantum trajectory in phase space.

We now show that a single particle described by a minimum uncertainty wave packet obeys exactly the Hamilton equations of motion within one band, in the classical limit to be specified below. Let us consider a normalized minimum uncertainty Gaussian wave packet, which we denote by $\langle \mathbf{x}|\mathbf{p}_c,\mathbf{q}_c\rangle$ (also often referred to as coherent state labeled by $\mathbf{p}_c$ and $\mathbf{q}_c$). Coherent states have the property that they are overcomplete:

$$\langle \mathbf{x}|\mathbf{p}_c,\mathbf{q}_c\rangle = \frac{1}{(2\pi)^{3/4}\Delta^{3/2}} \exp\left\{ \frac{-(\mathbf{x}-\mathbf{q}_c)^2}{4\Delta^2} + \frac{i\mathbf{p}_c}{\hbar}\cdot\mathbf{x} \right\} . \tag{52}$$

Upon taking the Weyl transform of this wave packet $\langle \mathbf{x}|\mathbf{p}_c,\mathbf{q}_c\rangle$, and taking the continuum limit, the result is the minimum uncertainty Wigner wave packet or the minimal WDF (MWDF), denoted by $f_W^M(\mathbf{p},\mathbf{q};\mathbf{p}_c,\mathbf{q}_c)$, given by the following expression:

$$f_W^M(\mathbf{p},\mathbf{q};\mathbf{p}_c\mathbf{q}_c) = \left[\frac{2}{h}\right]^3 \exp\left\{\frac{-(\mathbf{q}-\mathbf{q}_c)^2}{2\Delta^2}\right\} \times \exp\left\{\frac{-2\Delta^2(\mathbf{p}-\mathbf{p}_c)^2}{\hbar^2}\right\} . \tag{53}$$

Note that in the limit $\hbar\to 0$, $\Delta\to 0$, such $\hbar/\Delta\to 0$ as well (in the minimum uncertainty case, $\Delta=\sqrt{\hbar/2}$ and $\hbar/\Delta=\sqrt{2\hbar}\to 0$ if $\hbar\to 0$), the MWDF is just a representation of the δ function. Therefore, in this classical limit, we have the Hamilton equation of motion

$$\frac{d\langle \hat{\mathbf{P}}(t)\rangle_n}{dt} = -\frac{\partial H_n(\mathbf{p}_c,\mathbf{q}_c)}{\partial \mathbf{q}_c} , \tag{54}$$

$$\frac{d\langle \hat{\mathbf{Q}}(t)\rangle_n}{dt} = \frac{\partial H_n(\mathbf{p}_c,\mathbf{q}_c)}{\partial \mathbf{p}_c} , \tag{55}$$

describing the classical equation of motion in one band. Therefore, the center coordinates of the MWDF obey the classical Hamilton equation. In what follows, we will simply refer to the center coordinates in phase space as the "dynamical variables" $\mathbf{p}_c$ and $\mathbf{q}_c$.

What we are interested in is the expected component ("weight") of the MWDF bearing the dynamical variables $\mathbf{p}_c$ and $\mathbf{q}_c$ (i.e., centered on $\mathbf{p}_c$ and $\mathbf{q}_c$) in an arbitrary QDF. We can calculate the expected "weight" in the usual manner as in calculating averages, namely

$$W(\mathbf{p}_c,\mathbf{q}_c,t) = \int f_w(\mathbf{p},\mathbf{q},t) f_W^M(\mathbf{p},\mathbf{q};\mathbf{p}_c,\mathbf{q}_c)\, d\mathbf{p}\, d\mathbf{q} . \tag{56}$$

We can view the $W(\mathbf{p}_c,\mathbf{q}_c)$ as the distribution of "dynamical variables" corresponding to any arbitrary QDF. Indeed, what we have defined as $W(\mathbf{p}_c,\mathbf{q}_c)$ can be shown to be the diagonal matrix element of the density-matrix operator $\hat{\rho}$ in the coherent-state representation,[19] i.e.,

$$W(\mathbf{p}_c,\mathbf{q}_c,t) = \langle \mathbf{p}_c,\mathbf{q}_c|\hat{\rho}(t)|\mathbf{p}_c,\mathbf{q}_c\rangle , \tag{57}$$

which is clearly non-negative because the density matrix is a positive-definite, trace-class operator. The above results are well-known in the coherent-state phase-space formulation of quantum mechanics, aimed at making calculations which correspond to the classical analogs.[19] It has been shown that this so-called Gaussian smoothing renders the QDF positive definite, and yet maintains all quantum information, because the smoothing corresponds to a mere change of the operator-ordering scheme from that inherent in the QDF/Wigner approach.[20,21] The smoothed-out QDF is often called the Husimi distribution[22] function, and has been useful in the study of quantum tunneling and chaos in driven nonlinear quantum systems, by studying the structure of phase space.[12,16]

Related to the QDF (or WDF), it has some common properties, as expressed by the following relations:[19]

$$\langle \mathbf{p}\rangle = \int f_w(\mathbf{p},\mathbf{q})\mathbf{p}\, d\mathbf{p}\, d\mathbf{q} = \int W(\mathbf{p}_c,\mathbf{q}_c)\mathbf{p}_c\, d\mathbf{p}_c\, d\mathbf{q}_c , \tag{58}$$

$$\langle \mathbf{q}\rangle = \int f_w(\mathbf{p},\mathbf{q})\mathbf{q}\, d\mathbf{p}\, d\mathbf{q} = \int W(\mathbf{p}_c,\mathbf{q}_c)\mathbf{q}_c\, d\mathbf{p}_c\, d\mathbf{q}_c , \tag{59}$$

$$\langle \mathbf{p}_c^2\rangle = \langle \mathbf{p}^2\rangle + \frac{1}{2\hbar} , \tag{60}$$

$$\langle \mathbf{q}_c^2\rangle = \langle q^2\rangle + \frac{1}{2\hbar} . \tag{61}$$

However, $W(\mathbf{p}_c,\mathbf{q}_c)$ is a normalized quasidistribution, since the integral over $\mathbf{p}_c$ or $\mathbf{q}_c$ does not lead to distribution of coordinates or momenta, i.e.,

$$\int W(\mathbf{p}_c,\mathbf{q}_c)\, d\mathbf{p}_c = \left[\frac{h}{2}\right]^3 \left[\frac{\pi\hbar^2}{2\Delta^2}\right]^{3/2} \int \rho(\mathbf{q}) \exp\left\{\frac{-(\mathbf{q}-\mathbf{q}_c)^2}{2\Delta^2}\right\} d\mathbf{q} , \tag{62}$$

and similarly,

$$\int W(\mathbf{p}_c,\mathbf{q}_c)\, d\mathbf{q}_c = \left[\frac{h}{2}\right]^3 (\pi 2\Delta^2)^{3/2} \int \rho(\mathbf{p}) \exp\left\{\frac{-2\Delta^2(\mathbf{p}-\mathbf{p}_c)^2}{\hbar^2}\right\} d\mathbf{p} , \tag{63}$$

with

$$\int W(\mathbf{p}_c,\mathbf{q}_c)\, d\mathbf{p}_c\, d\mathbf{q}_c = 1 , \tag{64}$$

which show that the smoothed distribution function $W(\mathbf{p}_c,\mathbf{q}_c)$ does not lead directly to distributions of momenta or coordinates, but instead to a smoothed-out distribution of momenta or coordinates. On the other hand, we have found that in most cases in our numerical RTD simulations, the distribution of momenta or coordinates is often quite smooth, even if the full QDF is violently oscillating. In these cases, the Gaussian smoothing function can simply act like a δ function, and we can write the following approximations:

$$\int W(\mathbf{p}_c,\mathbf{q}_c)\, d\mathbf{p}_c \cong \rho(\mathbf{q}_c) , \tag{65}$$

$$\int W(\mathbf{p}_c,\mathbf{q}_c)\, d\mathbf{q}_c \cong \rho(\mathbf{p}_c) . \tag{66}$$

The above approximations allow us to treat the smoothed-out function $W(\mathbf{p}_c,\mathbf{q}_c)$ as a true probability distribution function. These approximations are made here only to illustrate these salient features of $W(\mathbf{p}_c,\mathbf{q}_c)$, but they are not required for the full analysis of the problem.

Moreover, in a manner similar to the treatment of the QDF transport equation, we can apply the Liouville representation for calculating steady-state trajectories in phase space by identifying the smoothed-out QDF transport equation with

$$\frac{\partial W(\mathbf{p}_c,\mathbf{q}_c,t)}{\partial t} = -\dot{\mathbf{q}}_c\cdot\nabla_{q_c} W(\mathbf{p}_c,\mathbf{q}_c,t) - \dot{\mathbf{p}}_c\cdot\nabla_{p_c} W(\mathbf{p}_c,\mathbf{q}_c,t) \ . \tag{67}$$

In the Liouville representation, it becomes more appealing physically to interpret the evolution of $W(\mathbf{p}_c,\mathbf{q}_c,t)$ as due to the propagation of quantum trajectories in dynamical phase space, where $W(\mathbf{p}_c,\mathbf{q}_c,t)$ satisfies the Liouville theorem

$$\frac{dW(\mathbf{p}_c,\mathbf{q}_c,t)}{dt}=0 \ . \tag{68}$$

Therefore, for steady-state situations the contour lines of $W(\mathbf{p}_c,\mathbf{q}_c,t)$ give the description of the quantum particle trajectories; these reduce to the Wigner trajectories, which were calculated in Refs. 11 and 17 for a relatively smooth QDF (or WDF). This discussion serves to justify the association made in Refs. 11 and 17 of Wigner trajectories to quantum particle trajectories.

For calculating time-evolving trajectories from a dynamical equation of motion, we can use the phase-space fluid representation by identifying the time-evolution equation for $W(\mathbf{p}_c,\mathbf{q}_c,t)$ with,

$$\frac{\partial W(\mathbf{p}_c,\mathbf{q}_c,t)}{\partial t} = -\nabla_c\cdot\mathbf{J}_c(\mathbf{p}_c,\mathbf{q}_c,t) \ , \tag{69}$$

where

$$\nabla_c \equiv [\nabla_{p_c},\nabla_{q_c}] \ , \tag{70}$$

$$\mathbf{J}_c=[\mathbf{J}_{p_c}(\mathbf{p}_c,\mathbf{q}_c,t),\mathbf{J}_{q_c}(\mathbf{p}_c,\mathbf{q}_c,t)] \ , \tag{71}$$

$$-\nabla_{q_c}\cdot\mathbf{J}_{q_c}(\mathbf{p}_c,\mathbf{q}_c,t)=\frac{1}{i\hbar}\left\langle \mathbf{p}_c,\mathbf{q}_c \left| \left[\frac{\hat{\mathbf{P}}^2}{2m^*},\hat{\rho}\right] \right| \mathbf{p}_c,\mathbf{q}_c \right\rangle \ , \tag{72}$$

$$-\nabla_{p_c}\cdot\mathbf{J}_{p_c}(\mathbf{p}_c,\mathbf{q}_c,t)=\frac{1}{i\hbar}\langle \mathbf{p}_c,\mathbf{q}_c|[\hat{V},\hat{\rho}]|\mathbf{p}_c,\mathbf{q}_c\rangle + \frac{1}{i\hbar}\langle \mathbf{p}_c,\mathbf{q}_c|\hat{C}|\mathbf{p}_c,\mathbf{q}_c\rangle \ . \tag{73}$$

We have included the collision operator $\hat{C}$, taken in the relaxation-time approximation, in the definition of the smoothed-out phase-space current in the dynamical phase space. By using the last two equalities, which serve to define the velocity $\dot{\mathbf{q}}_c$, and the force $\dot{\mathbf{p}}_c$, we may now interpret the evolution of $W(\mathbf{p}_c,\mathbf{q}_c,t)$ as due to the propagation of quantum trajectories in dynamical phase space. However, the smoothed-out distribution does not satisfy the Liouville theorem.

As indicated before, in general $W(\mathbf{p}_c,\mathbf{q}_c,t)$ cannot be considered as a true probability distribution. On the other hand, the continuity equation still allows us to regard the smoothed non-negative distribution as leading to a conserved density in phase space. We may therefore interpret the smoothed distribution $W(\mathbf{p}_c,\mathbf{q}_c,t)$ as the density for a conserved quantum fluid flowing in phase space, i.e., the evolution of $W(\mathbf{p}_c,\mathbf{q}_c,t)$ may still be viewed as due to the propagation of quantum trajectories in phase space. The calculational difficulties arise from the fact that the resulting particle trajectories are no longer generated by the Hamiltonian dynamical equations. What we need is a generalization of the fluid flow equations, in the same manner that was attempted before for the QDF transport equation.

To obtain the quantum trajectories in phase space, we need to calculate the velocity field $\mathbf{v}_{p_c}(\mathbf{p}_c,\mathbf{q}_c,t)$ and $\mathbf{v}_{q_c}(\mathbf{p}_c,\mathbf{q}_c,t)$. Using this velocity field, the quantum particle trajectories which govern the evolution of the smoothed density are obtained as solutions to the following generalized dynamical equations:

$$\frac{d\mathbf{p}_c}{dt}=\mathbf{v}_{p_c}(\mathbf{p}_c,\mathbf{q}_c,t) \ , \tag{74}$$

$$\frac{d\mathbf{q}_c}{dt}=\mathbf{v}_{q_c}(\mathbf{p}_c,\mathbf{q}_c,t) \ . \tag{75}$$

Numerically, the movement of the trajectory in phase space is described by the following algorithm:

$$(\mathbf{p}_c,\mathbf{q}_c,t+\delta t)=\left\{\frac{\mathbf{v}(\mathbf{p}_c^0,\mathbf{q}_c^0,t)+\mathbf{v}(\mathbf{p}_c^0,\mathbf{q}_c^0,t+\delta t)}{2}\right\} \times\delta t+(\mathbf{p}_c^0,\mathbf{q}_c^0,t) \ . \tag{76}$$

One can also study the structure of phase space by means of trajectories using "stroboscopic techniques," i.e., by calculating the contour lines of $W(\mathbf{p}_c,\mathbf{q}_c,t)$ at various instants of time.

The major task therefore lies in calculating the velocity field. We will discuss this in more detail here. This velocity field in phase space can be defined in terms of the flux density $\mathbf{J}(\mathbf{p}_c,\mathbf{q}_c,t)$ and the $W(\mathbf{p}_c,\mathbf{q}_c,t)$ as follows:

$$\mathbf{J}(\mathbf{p}_c,\mathbf{q}_c,t)=\mathbf{v}(\mathbf{p}_c,\mathbf{q}_c,t)W(\mathbf{p}_c,\mathbf{q}_c,t) \ , \tag{77}$$

where $W(\mathbf{p}_c,\mathbf{q}_c,t)$ is the result of smoothing the QDF (or WDF). Therefore the central task is in evaluating the flux density in phase space, $\mathbf{J}(\mathbf{p}_c,\mathbf{q}_c,t)$. This can be done in principle since the existence of well-defined $\mathbf{J}(\mathbf{p}_c,\mathbf{q}_c,t)$ is assured by the continuity equation. Indeed, the continuity equation and the velocity field govern the changes with time of $W(\mathbf{p}_c,\mathbf{q}_c,t)$, and lead to the violation of the Liouville theorem in classical mechanics. This is derived as follows. Let us write

$$\frac{dW(\mathbf{p}_c,\mathbf{q}_c,t)}{dt}=\frac{\partial W(\mathbf{p}_c,\mathbf{q}_c,t)}{\partial t}+\mathbf{v}\cdot\nabla W(\mathbf{p}_c\mathbf{q}_c,t) \ . \tag{78}$$

Using the continuity equation in lieu of the first term on

the right-hand side of Eq. (78), we obtain

$$\frac{dW(\mathbf{p}_c,\mathbf{q}_c,t)}{dt}=W(p_c,q_c,t)\nabla\cdot\mathbf{v}(\mathbf{p}_c,\mathbf{q}_c,t)\ . \tag{79}$$

One can see from the definition of $\mathbf{v}(\mathbf{p}_c,\mathbf{q}_c,t)$ that the divergence of the velocity field in phase space is nonzero in general, i.e., there is no conservation in phase-space volume. This is in contrast to the use of Liouville's theorem, where the Hamiltonian structure is such that the following holds:

$$\nabla\cdot\mathbf{v}=\frac{\partial^2 H}{\partial\mathbf{p}\partial\mathbf{q}}-\frac{\partial^2 H}{\partial\mathbf{p}\partial\mathbf{q}}\equiv 0\ . \tag{80}$$

The flux density in phase space can be determined from the QDF by using Eq. (1) and the continuity equation for the $W(\mathbf{p}_c,\mathbf{q}_c,t)$:

$$\mathbf{J}_{q_c}(\mathbf{p}_c,\mathbf{q}_c,t)=\int\frac{\mathbf{p}}{m}f_w(\mathbf{p},\mathbf{q},t)f_W^M(\mathbf{p},\mathbf{q};\mathbf{p}_c,\mathbf{q}_c)d\mathbf{p}\,d\mathbf{q}\ , \tag{81}$$

$$\begin{aligned}J_{p_c^\alpha}(\mathbf{p}_c,\mathbf{q}_c,t)=&\frac{1}{h^3}\int d\mathbf{p}'d\boldsymbol{\nu}\left\{V\left[\mathbf{q}-\frac{\boldsymbol{\nu}}{2}\right]-V\left[\mathbf{q}+\frac{\boldsymbol{\nu}}{2}\right]\right\}\Big/\nu^\alpha\\&\times\cos\left[\frac{(\mathbf{p}-\mathbf{p}')}{\hbar}\cdot\boldsymbol{\nu}\right]f_w(\mathbf{p}',\mathbf{q},t)f_W^M(\mathbf{p},\mathbf{q};\mathbf{p}_c,\mathbf{q}_c)d\mathbf{p}d\mathbf{q}\\&-\frac{1}{\tau}\int_0^{p_\alpha}dp'_\alpha\left[\frac{\rho(\mathbf{q},t)}{\rho_0(\mathbf{q})}f_0(\mathbf{p}',\mathbf{q})-f_W(\mathbf{p}',\mathbf{q},t)\right]f_W^M(\mathbf{p},\mathbf{q};\mathbf{p}_c,\mathbf{q}_c)d\mathbf{p}\,d\mathbf{q}\ .\end{aligned} \tag{82}$$

The virtue of the approach taken here in studying the phase-space structure is that we have avoided the direct numerical solution of the smoothed distribution $W(\mathbf{p}_c,\mathbf{q}_c,t)$ whose integrodifferential equation is more difficult to solve than the QDF transport equation. It is more preferable that the smoothing procedure and the calculation of quantum trajectories be performed as a processor of the numerically obtained QDF or WDF, with a small ac signal component applied at the drain boundary. The last point needs to be stressed, since this is the essence of the method proposed in this paper for studying the structure of phase space. This approach consists of the following procedure.

(1) Numerical solution of the QDF transport equation of the RTD using a subsidiary open boundary condition, as described in Refs. 3 and 11.

(2) Processing the numerically obtained QDF solution, e.g., using Gaussian smoothing, to calculate other quantities of interest, such as the current flux densities in "dynamical" phase space and the velocity fields and map the time-evolving trajectories in order to study the structure of phase space.

There are two ways to characterize the trajectories: (a) By means of "stroboscopic techniques," calculating the surface contours of the Husimi distributions at various instants of time. This is conveniently done in the Liouville representation. (b) Solving the general "phase-space fluid" dynamical equation of motion, Eqs. (74) and (75), in the phase-space fluid representation.

The approach proposed here should allow one to study the respective contributions of tunneling and nontunneling trajectories to the current flux. The study of the separation between tunneling and nontunneling trajectories will naturally lead to a division of phase space, with a dynamically changing separation boundary. This will lead to a "classical" division of the current corresponding to the tunneling-transport and displacement currents. Moreover, the detailed dynamical study of the tunneling component would reveal the complex dynamical nature of the quantum inductance, L. Clearly, the BJ equivalent-circuit model for the RTD is suggested by the expected dichotomy of phase space into the "reactive tunneling component" and "displacement component."

V. CONCLUDING REMARKS

In this paper, we have demonstrated that the BJ equivalent-circuit model for the RTD goes a long way toward characterizing the different fundamental behavior of a double-barrier nanostructure, as revealed by the numerical quantum transport simulations. The results obtained here lend support to the accuracy of the BJ equivalent-circuit model of a RTD at fixed bias (and low-frequency bias at the drain), as well as confirming the validity of the high-frequency equivalent-circuit model of the RTD introduced in this paper, which incorporates a smaller series inertial inductance in addition to the quantum inductance. These results also serve to invalidate a claim made without any reservation that no LRC circuitry can simulate the complicated frequency dependence of the admittance in the linear-response regime.[8] It is worthwhile to reiterate that the BJ equivalent-circuit model is subtle and basic to the characterization of the different behavior of the RTD obtained from quantum transport numerical simulations. Indeed, the model presented here dispels the discrepancy in the reactive behavior of the two earlier numerical simulations of the small ac signal response as two different special cases of the parametrization of the BJ equivalent-circuit model for the RTD. Thus the discrepancy between the reactive behaviors found by Frensley[5] and Kluksdahl *et al.*[6] is resolved. Moreover, the exact role of electron inertia in the high-frequency behavior of the RTD is clarified in this paper.

For the case when linear-response approximation breaks down, as would be the case when the correspond-

ing parametrization of the BJ equivalent-circuit model corresponds to the parametrization used by BJ to explain the plateaulike behavior of the I-V characteristic, then a nonperturbative-response scheme is required. In this paper, we propose to study this problem by three methods which are expected to complement each other.

The first method is the use of the equivalent-circuit model of the RTD, biased in the NDR region, by incorporating nonlinear terms in the $i(v)$ characteristic of the nonlinear resistor. A host of nonlinear behaviors, including enhancement and/or quenching of the intrinsic oscillatory "limit-cycle" current behavior, as a function of the frequency of the exciting signal, would be quite interesting to investigate.

The second method is through the study of the fundamental quantum transport equation in the presence of a time-dependent but position-independent electric field throughout the device. This type of applied bias is a standard approach in analytical transport theory. The virtue of this method is that it can reveal nonperturbative fundamental effects due to a small ac signal. Indeed, in this paper we have shown that a time-dependent transformation of phase space can be used to reduce the problem to a problem of the absence of the applied ac field, which has been subjected to a time-dependent numerical simulations in Refs. 3 and 11. The only difference is that the double-barrier potential in the moving phase space acquires time as a parameter, effectively executing a vibrating motion in the moving coordinates. Nevertheless, the customary numerical technique can be used to study this problem. Moreover, transformation back to the laboratory frame explicitly reveals another component of the time dependence, which is effectively due to the "vibrating current density wave (as function of position)" across the device.

The third method formulated here relies on a numerical approach. It is based on a detailed study of the "classical" structure of phase space. It extends the previous numerical approach to a time-dependent ac bias at the drain. In this approach, it is assumed that a bias in the middle of the NDR region, with a small ac component, is applied at the drain in the customary time-dependent numerical simulation. The numerically obtained time-dependent QDF solutions are then processed to calculate various quantities, as routinely done before,[3] with an additional procedure for Gaussian smoothing of the QDF in order to calculate quantum trajectories, velocity fields, and current fluxes. Although this procedure is expected to be computer processing intensive, it will open up interesting regimes of investigation of the nonlinear properties of quantum-based devices, bringing additional nonlinear quantum effects to the fore, and ushering new applications of these nonlinear quantum phenomena. Indeed, the use of the Husimi distribution has already made it possible to study some interesting properties of quantum tunneling and chaos in a driven anharmonic oscillator,[12,16] showing interesting parametrically controlled tunneling rates. Application of Husimi distribution to technologically important open systems has, to our knowledge, never been discussed in the literature; this paper serves to make a beginning in this direction.

ACKNOWLEDGMENT

The financial support from the Office of Naval Research is gratefully acknowledged.

APPENDIX A: TRANSFORMATION OF THE QDF TRANSPORT EQUATION

In the presence of many-body effects, the proper starting point in the derivation of Eq. (37) is the exact QDF transport equation derived by one of the authors (Ref. 11), using the lattice Weyl-Wigner formulation of the quantum dynamics (LWWFQD) of electrons in solids. In the continuum limit of the LWWFQD, the time-evolution equation for the single-particle density matrix in phase space or the QDF, $\rho^{<}(\mathbf{p},E,\mathbf{q},t)$, is given as [writing $\mathbf{p}=(\mathbf{p},E),\mathbf{q}=(\mathbf{q},t)$] (Ref. 11)

$$
\begin{aligned}
-\frac{\hbar}{i}\frac{\partial}{\partial t}\rho^{<}(\mathbf{p},E,\mathbf{q},t)=&\frac{1}{\left[\frac{h}{2}\right]^8}\int dp'dq'K^{s}_{\tilde{H}}(p,q;p',q')\rho^{<}(p',q')+\frac{1}{(h/2)^8}\int dp'dq'K^{s}_{\Sigma^{<}}(p,q;p',q')(-i)\mathrm{Re}G^{r}(p',q')\\
&-\frac{1}{\left[\frac{h}{2}\right]^8}\int dp'dq'K^{c}_{\Sigma^{<}}(p,q;p',q')(-i)\mathrm{Im}G^{r}(p',q')\\
&-\frac{1}{\left[\frac{h}{2}\right]^8}\int dp'dq'K^{c}_{\Gamma}(p,q';p',q')\rho^{<}(p',q') \qquad \text{(A1)}
\end{aligned}
$$

where $\tilde{H}=H+\mathrm{Re}\Sigma^{r}$, and the integral kernels are defined by

$$
K^{s}_{a}(p,q,p',q')=\int du\,dv\left\{\exp\left[\frac{2i}{\hbar}\{(q-q')\cdot u+(p-p')\cdot v\}\right]\{a(p+q,q-v)-a(p-u,q+v)\}\right\}, \qquad \text{(A2)}
$$

$$
K^{c}_{a}(p,q;p',q')=\int du\,dv\exp\left\{\frac{2i}{\hbar}[(q-q')\cdot u+(p-p')v]\right\}\{a(p+q,q-v)+a(p-u,q+v)\}\ . \qquad \text{(A3)}
$$

The time-evolution equation for $G^r(\mathbf{p},E,\mathbf{q},t)$ may also be given as

$$-\frac{\hbar}{i}\frac{\partial}{\partial t}G^r(\mathbf{p},E,\mathbf{q},t)=\frac{1}{(h^4)^2}\int dp'dq'K^s_{H+\Sigma^r}(p,q;p'q')G^r(p',q') \ . \tag{A4}$$

To simplify the nonperturbative calculation of the small ac signal response, we will neglect the second term of Eq. (A1), and take into account the last two terms in the leading terms of the expansion in powers of $\hbar$. The result is an equation for the Wigner-distribution function which includes leading collision terms, given by

$$-\frac{\hbar}{i}\frac{\partial}{\partial t}\rho^<(\mathbf{p},E,\mathbf{q},t)=\frac{1}{(h^4)^2}\int dp'dq'K^s_{\tilde{H}}(p,q;p',q')\rho^<(p',q')+[\Sigma^<(p,q,t)A(p,q,t)-\Gamma(p,q,t)G^<(p,q,t)] \ . \tag{A5}$$

where $H=\mathbf{p}^2/2m+V(\mathbf{q})-\mathbf{f}(t)\cdot\mathbf{q}$. The time-dependent perturbation is $\mathbf{f}(t)\cdot\mathbf{q}$ as the position-independent but time-dependent external electric field. Evaluating the integral in Eq. (A5), using H in the effective-mass approximation given above, we end up with the following expression:

$$\begin{aligned}\frac{\partial\rho^<}{\partial t}(\mathbf{p},E,\mathbf{q},t)=&\frac{-\mathbf{p}}{m}\cdot\nabla_q\rho^<(\mathbf{p},E,\mathbf{q},t)+\frac{1}{\hbar}\left[\frac{h}{2}\right]^3\int d\mathbf{p}'d\boldsymbol{\nu}\sin\left[\frac{2}{\hbar}(\mathbf{p}-\mathbf{p}')\cdot\boldsymbol{\nu}\right]\\&\times[V(\mathbf{q}-\boldsymbol{\nu})-V(\mathbf{q}+\boldsymbol{\nu})]\rho^<(\mathbf{p}',E,\mathbf{q},t)\\&-\mathbf{f}(t)\cdot\nabla_{\mathbf{p}}\rho^<(\mathbf{p},E,\mathbf{q},t)-\mathbf{q}\cdot\dot{\mathbf{f}}(t)\frac{\partial}{\partial E}\rho^<(\mathbf{p},E,\mathbf{q},t)\\&-\frac{i}{\hbar}\{\Sigma^<(\mathbf{p},\mathbf{E})A(\mathbf{p},E)-\Gamma(\mathbf{p},E)G^<(\mathbf{p},E\mathbf{q},t)\}\end{aligned} \tag{A6}$$

where we assume that the self-energies and spectral functions are independent of time and position.

We can eliminate the explicit appearance of the driving term, $\mathbf{f}(t)$, and its time derivative from the last equation by making the following transformation in phase space:

$$\mathbf{p}'=\mathbf{p}_0+\int\mathbf{f}(t'')dt'' \ , \tag{A7}$$

$$E'=E_0+\mathbf{q}_0\cdot\mathbf{f}(t') \ , \tag{A8}$$

$$\mathbf{q}'=\mathbf{q}_0+\xi(t') \ , \tag{A9}$$

where

$$\mathbf{p}_0=\mathbf{p} \ , \tag{A10}$$

$$E_0=E \ , \tag{A11}$$

$$\mathbf{q}_0=\mathbf{q} \ , \tag{A12}$$

$$\dot{\xi}(t')=\int^{t'}\mathbf{f}(t'')dt'' \ , \tag{A13}$$

$$t'=t \ . \tag{A14}$$

In terms of the moving phase spaces (primed variables), we have

$$\begin{aligned}\frac{\partial}{\partial t'}\rho^<(\mathbf{p}',E',\mathbf{q}',t')=&-\frac{\mathbf{p}'}{m}\cdot\nabla_{q'}\rho^<(\mathbf{p}',E',\mathbf{q}',t')+\frac{1}{\hbar\left[\frac{h}{2}\right]^3}\int d\mathbf{p}''d\boldsymbol{\nu}\sin\left[\frac{2}{\hbar}(\mathbf{p}'-\mathbf{p}'')\cdot\boldsymbol{\nu}\right]\\&\times\{V[\mathbf{q}'-\xi(t')-\boldsymbol{\nu}]-V[\mathbf{q}'-\xi(t')+\boldsymbol{\nu}]\}\rho^<(\mathbf{p}'',E',\mathbf{q}',t')\\&-\frac{i}{\hbar}\{\Sigma^<(\mathbf{p}',E')A(\mathbf{p}',E')-\Gamma(\mathbf{p}',E')G^<(\mathbf{p}',E',\mathbf{q}',t')\} \ .\end{aligned} \tag{A15}$$

Applying the relaxation-time approximation to the last term, we have

$$-\frac{i}{\hbar}\int dE'\{\Sigma^<(\mathbf{p}',E')A(\mathbf{p}',E')-\Gamma(\mathbf{p}',E')G^<(\mathbf{p}',E',\mathbf{q}',t')\}=\frac{1}{\tau}\left\{\frac{\rho(\mathbf{q}',t')}{\rho_0(\mathbf{q}')}f_0(\mathbf{p}',\mathbf{q}')-f_w(\mathbf{p}',\mathbf{q}',t')\right\} \ . \tag{A16}$$

Therefore, by integrating with respect to the energy variable, and noting that $dE=dE'$, we finally obtain

$$\frac{\partial}{\partial t'}f_w(\mathbf{p}',\mathbf{q}',t')=-\frac{\mathbf{p}'}{m}\cdot\nabla_{\mathbf{q}'}f_w(\mathbf{p}',\mathbf{q}',t)+\frac{1}{\hbar\left[\frac{h}{2}\right]^3}\int d\mathbf{p}''d\boldsymbol{\nu}\sin\left[\frac{2}{\hbar}(\mathbf{p}'-\mathbf{p}'')\cdot\boldsymbol{\nu}\right]$$
$$\times\{V[\mathbf{q}'-\boldsymbol{\xi}(t')-\boldsymbol{\nu}]-V[\mathbf{q}'-\boldsymbol{\xi}(t')+\boldsymbol{\nu}]\}f_w(\mathbf{p}'',\mathbf{q}',t')$$
$$+\frac{1}{\tau}\left\{\frac{\rho(\mathbf{q}',t')}{\rho_0(\mathbf{q}')}f_0(\mathbf{p}',\mathbf{q}')-f_w(\mathbf{p}',\mathbf{q}',t')\right\}. \tag{A17}$$

In the absence of the collision terms, the above result can of course be obtained by starting with the equation for the single-particle density-matrix operator

$$\frac{\partial\hat{\rho}}{\partial t}=\frac{i}{\hbar}[\hat{H},\hat{\rho}] \tag{A18}$$

instead of Eq. (A1).

APPENDIX B: DERIVATION OF SMOOTHED-OUT CURRENT FLUXES

The time-evolution equation for $W(\mathbf{p}_c,\mathbf{q}_c,t)$ can readily be deduced by smoothing Eq. (1). The result is given by

$$\frac{\partial W(\mathbf{p}_c,\mathbf{q}_c,t)}{\partial t}=-\int d\mathbf{p}\,d\mathbf{q}\left\{\frac{\mathbf{p}}{m}\cdot\nabla_{\mathbf{q}}f_w(\mathbf{p},\mathbf{q},t)f_w^M(\mathbf{p},\mathbf{q};p_c\mathbf{q}_c)\right\}$$
$$+\frac{1}{\hbar\left[\frac{h}{2}\right]^3}\int d\mathbf{p}\,d\mathbf{q}\left\{\int d\mathbf{p}'d\boldsymbol{\nu}\sin\left[\frac{2}{\hbar}(\mathbf{p}-\mathbf{p}')\cdot\boldsymbol{\nu}\right][V(\mathbf{q}-\boldsymbol{\nu})-V(\mathbf{q}+\boldsymbol{\nu})]f_w(\mathbf{p}',\mathbf{q},t)f_w^M(\mathbf{p},\mathbf{q};\mathbf{p}_c,\mathbf{q}_c)\right\}$$
$$+\frac{1}{\tau}\int d\mathbf{p}\,d\mathbf{q}\left\{\frac{\rho(\mathbf{q},t)}{\rho_0(\mathbf{q})}f_0(\mathbf{p},\mathbf{q})-f_w(\mathbf{p},\mathbf{q},t)\right\}f_w^M(\mathbf{p},\mathbf{q};p_c,\mathbf{q}_c)$$

We are interested in transforming the above equation to the form of Eq. (69). In order to do this, we make the transformation $\mathbf{q}=\tilde{\mathbf{q}}+\mathbf{q}_c$ to the first term, use $\nabla_{\mathbf{q}}=\nabla_{\mathbf{q}_c}$ and transfer $\nabla_{\mathbf{q}_c}$ out of the integral sign. We are left with the form $\nabla_{q_c}\cdot\mathbf{J}_{q_c}(\mathbf{p}_c,\mathbf{q}_c,\mathbf{t})$. This define $\mathbf{J}_{\mathbf{q}_c}(\mathbf{p}_c,\mathbf{q}_c,t)$ given by Eq. (81). Similarly, for the second and third term, first let $\mathbf{p}=\tilde{\mathbf{p}}+\mathbf{p}_c$, and recast these terms as gradient terms with respect to $\mathbf{p}_c$, i.e., $\nabla_{p_c}\cdot\mathbf{J}_{p_c}(\mathbf{p}_c,\mathbf{q}_c,t)$. The result serves to define $\mathbf{J}_{p_c}(\mathbf{p}_c,\mathbf{q}_c,t)$ as given by Eq. (82).

[1]V. J. Goldman, D. C. Tsui, and J. E. Cunningham, Phys. Rev. Lett. **58**, 1256 (1987).
[2]T. C. L. G. Sollner, Phys. Rev. Lett. **59**, 1622 (1987).
[3]K. L. Jensen and F. A. Buot, Phys. Rev. Lett. **66**, 1078 (1991).
[4]F. A. Buot and K. L. Jensen, Int. J. Comp. Math. Elec. Electron. Eng., **COMPEL 10**, 241 (1991).
[5]W. R. Frensley, Rev. Mod. Phys. **62**, 765 (1990). In this paper, the author corrects his earlier work [Appl. Phys. Lett. **51**, 448 (1987)] on the reactive behavior of RTD.
[6]N. C. Kluksdahl, A. M. Kriman, D. K. Ferry, and C. Ringhofer, IEEE Electron Device Lett. **9**, 457 (1988).
[7]R. Landauer, Phys. Scr. **T42**, 112 (1992).
[8]Y. Fu and C. Dudley, Phys. Rev. Lett. **70**, 65 (1993).
[9]L. Y. Chen and C. S. Ting, Phys. Rev. Lett. **64**, 3159 (1990).
[10]W. Cai and M. Lax, Phys. Rev. B **47**, 4096 (1993).
[11]F. A. Buot and K. L. Jensen, Phys. Rev. B **42**, 9429 (1990).
[12]G. J. Milburn, Phys. Rev. A **39**, 2749 (1989).
[13]R. E. Salvino and F. A. Buot, J. Appl. Phys. **72**, 5975 (1992).
[14]W. H. Press, B. P. Flannery, S. A. Teukolsky, and W. T. Vetterling, *Numerical Recipes: The Art of Scientific Computing* (Cambridge University Press, New York, 1986).
[15]G. C. Atallah and J. Geer, Int. J. Non-Linear Mech. **22**, 439 (1987). See also J. Guckenheimer and P. Holmes, *Nonlinear Oscillations, Dynamical Systems and Bifurcations of Vector Fields* (Springer-Verlag, New York, 1983).
[16]W. A. Lin and L. E. Ballantine, Phys. Rev. A **45**, 3637 (1992); Phys. Rev. Lett. **65**, 2927 (1990).
[17]K. L. Jensen and F. A. Buot, IEEE Trans. Electron Devices **38**, 2337 (1991).
[18]F. A. Buot, Phys. Rev. A **33**, 2544 (1986).
[19]A. K. Rajagopal, Phys. Rev. A **27**, 558 (1983). The class of Gaussian smoothing introduced in this paper is related to the coherent state of quantum optics. See also A. K. Rajagopal, Phys. Rev. A **26**, 2977 (1982).
[20]K. E. Cahill and R. J. Glauber, Phys. Rev. **177**, 1882 (1969).
[21]G. S. Agarwal and E. Wolf, Phys. Rev. D **2**, 2161 (1970).
[22]K. Takahashi, J. Phys. Soc. Jpn. **55**, 762 (1986); **55**, 1443 (1986).